Engineering 15 (2022) 78–88

Contents lists available at ScienceDirect

Engineering

journal homepage: www.elsevier.com/locate/eng

Research
Antimicrobial Resistance—Article

Three-Year Consecutive Field Application of Erythromycin Fermentation Residue Following Hydrothermal Treatment: Cumulative Effect on Soil Antibiotic Resistance Genes

Ziming Han [a,b], Haodi Feng [a], Xiao Luan [a], Yunpeng Shen [c], Liren Ren [c], Liujie Deng [c], D.G. Joakim Larsson [d], Michael Gillings [e], Yu Zhang [a,b,*], Min Yang [a,b]

[a] State Key Laboratory of Environmental Aquatic Chemistry, Research Center for Eco-Environmental Sciences, Chinese Academy of Sciences, Beijing 100085, China
[b] University of Chinese Academy of Sciences, Beijing 100049, China
[c] State Environmental Protection Engineering Center for Harmless Treatment and Resource Utilization of Antibiotic Residues, Khorgos 835007, China
[d] Institute for Biomedicine & the Centre for Antibiotic Resistance Research, University of Gothenburg, Göteborg SE-413 46, Sweden
[e] Australian Research Council (ARC) Centre of Excellence in Synthetic Biology, Department of Biological Sciences, Faculty of Science and Engineering, Macquarie University, Sydney, NSW 2109, Australia

ARTICLE INFO

Article history:
Received 15 December 2021
Revised 23 April 2022
Accepted 24 May 2022
Available online 11 June 2022

Keywords:
Pharmaceutical manufacturing
Resistome
Antibiotic
Risk assessment
Remediation
Land application

ABSTRACT

Fermentation-based antibiotic production results in abundant nutrient-rich fermentation residue with high potential for recycling, but the high antibiotic residual concentration restricts its usefulness (e.g., in land application as organic fertilizer). In this study, an industrial-scale hydrothermal facility for the treatment of erythromycin fermentation residue (EFR) was investigated, and the potential risk of the long-term soil application of treated EFR promoting environmental antibiotic resistance development was evaluated. The treatment effectively removed bacteria and their DNA, and an erythromycin removal ratio of up to approximately 98% was achieved. The treated EFR was utilized as organic fertilizer for consecutive field applications from 2018 to 2020, with dosages ranging from 3750 to 15 000 kg·hm^{-2}, resulting in sub-inhibitory levels of erythromycin (ranging from 0.83–76.00 μg·kg^{-1}) in soils. Metagenomic shotgun sequencing was then used to characterize the antibiotic resistance genes (ARGs), mobile genetic elements (MGEs), and bacterial community composition of the soils. The soil ARG abundance and diversity did not respond to the treated EFR application in the first year, but gradually changed in the second and third year of application. The highest fold change in relative abundance of macrolide–lincosamide–streptogramin (MLS) and total ARGs were 12.59 and 2.75 times, compared with the control (CK; without application), respectively. The soil MGEs and taxonomic composition showed similar temporal trends to those of the ARGs, and appeared to assist in driving increasing ARG proliferation, as revealed by correlation analysis and structural equation models (SEMs). The relative abundance of particular *erm* resistance genes (RNA methyltransferase genes) increased significantly in the third year of treated EFR application. The close association of *erm* with MGEs suggested that horizontal gene transfer played a critical role in the observed *erm* gene enrichment. Metagenomic binning results demonstrated that the proliferation of *mac* gene-carrying hosts was responsible for the increased abundance of *mac* genes (efflux pump genes). This study shows that sub-inhibitory levels of erythromycin in soils had a cumulative effect on soil ARGs over time and emphasizes the importance of long-term monitoring for assessing the risk of soil amendment with treated industrial waste.

1. Introduction

Pharmaceutical manufacturing is a source of antibiotic pollution [1,2]. Antibiotic resistance genes (ARGs) and antibiotic-resistant bacteria (ARB) in environmental media can be promoted under antibiotic selective pressures caused by such pollution, in turn contributing to risk of accelerated resistance development and thus to public health risks [3]. In addition to the wastewater that is generated from antibiotic production, fermentation-based antibiotic-production processes lead to large volumes of byproducts from the bio-fermentation process, which mainly consist of

* Corresponding author.
E-mail address: zhangyu@rcees.ac.cn (Y. Zhang).

https://doi.org/10.1016/j.eng.2022.05.011

microbial biomass, fermentation substrate, and remaining antibiotic [4]. Because of its high organic-matter content, antibiotic fermentation residue (also called antibiotic mycelial residue) has potential as an organic fertilizer or soil amendment; however, the residual content of antibiotics restricts its use. It would be of apparent environmental and economic significance for the pharmaceutical industry if treated antibiotic fermentation residue could be used as a soil amendment. This has inspired the exploration of industrial operations that would enable such uses of fermentation residues.

Erythromycin is a macrolide antibiotic that is commonly used in human medicine and livestock production to treat infections caused by Gram-positive pathogenetic bacteria [5]. Erythromycin is reasonably persistent in the environment and has been detected in sewage sludge from wastewater treatment plants in the United States at a concentration of up to (62.8 ± 5.8) μg·kg^{-1} [6]. In addition, erythromycin is included in the watch-list under the Water Framework Directive of the European Union [7], due to its potential risk to ecosystem health. Although water concentrations of erythromycin above established effect levels rarely or never are demonstrated in surface waters as a result of use and excretion, risks cannot be excluded when safety factors are applied. The risk of resistance promotion was not part of the decision to include erythromycin in the abovementioned watch list; however, resistance selection could well be a more plausible consequence than other concerns, given that minimal inhibiting concentrations (MICs) for bacteria down to 16 μg·L^{-1} are reported, resulting in a predicted no effect concentration (PNEC) of 1 μg·L^{-1} in water [8]. In any case, it is challenging to translate effect levels from aquatic media to solid or semi-solid media [3].

Because of these potential risks, erythromycin fermentation residue (EFR) is a good model for investigating the efficacy and safety of industrial-scale treatment and subsequent soil application. It has been reported that many kinds of fermentative antibiotics (i.e., antibiotics produced by microbial fermentation) can be removed by temperature-enhanced hydrolysis from aquatic media, due to their easy-to-hydrolyze characteristics [9]. Hydrothermal pretreatment has recently been developed to remove antibiotics from wastewater, in order to mitigate the spread of antibiotic resistance in pilot and full-scale biological treatment for antibiotic production wastewater [10–12]. Hydrothermal treatment has the advantage of a relatively low cost and ease of industrial-scale application [13]; moreover, its ability to reduce erythromycin from EFR has been explored in a lab-scale study [14]. However, it is still a challenge for an antibiotic manufacturer to use hydrothermal treatment on semi-solid media such as fermentation residue. Consequently, testing industrial-scale hydrothermally treated EFR as a soil amendment should be a priority.

A reduced erythromycin concentration in the treated EFR is likely to reduce its selective pressure on soil microorganisms. A pot experiment found that the application of treated EFR led to erythromycin concentrations of 300 μg·kg^{-1} in soil, but that the abundance of erythromycin-related resistance genes (*erm*B, *erm*C, and *erm*X) was not increased after incubation for 49 d [15]. Similarly, a single soil application of treated EFR did not change the abundance of resistance genes [16]. In some contrast, a multiyear exposure experiment involving the direct addition of 10 mg·kg^{-1} of erythromycin to soil found that the erythromycin degradation rate increased over time, suggesting the proliferation of microorganisms capable of degrading the antibiotic [17]. Some erythromycin-related ARGs (only *msr*E and *mph*E have been measured) were enriched after the fourth year of exposure [18]. These results show a gradual, cumulative effect of long-term, repeated erythromycin applications on soil organisms and ARG abundance. Nevertheless, a comprehensive understanding of the microbiological mechanisms involved is still lacking.

Erythromycin concentrations in soils after the application of treated EFR have tended to be in the sub-inhibitory range for soil bacteria (ng·kg^{-1} to μg·kg^{-1} level) [15,16], and were found to be similar to antibiotic concentrations in the environment resulting from anthropogenic activities [19]. Residual antibiotics may affect the antibiotic resistome by inhibiting the growth of sensitive bacteria and promoting ARG dissemination by means of horizontal gene transfer [20], thereby contributing to the antibiotic resistance evolution [21,22]. In addition, the possible introduction of resistant bacteria present in the treated EFR to soils could contribute to such risks. Thus, to comprehensively assess the risk of promoting resistance evolution as a result of amending soils with treated EFR, it would be valuable to ① investigate long-term, consecutive land application, ② conduct time-series soil sampling, and ③ perform a systematic profiling of the antibiotic resistome and related determinants.

In this study, our aim was to provide field-based evidence of the impact of EFRs in soil ecosystems and to examine a real-world situation involving the disposal of pharmaceutical waste. The specific objectives were ① to investigate the remaining erythromycin in hydrothermally treated EFR and in amended soils receiving different dosages of treated EFR, ② to assess the cumulative impact on soil ARGs over time, and ③ to disentangle the contributions of the horizontal and vertical pathways of ARG dynamics in soils. To achieve this, we examined the soil application of hydrothermally treated EFR sourced from an erythromycin manufacturer. The treated EFR was used as organic fertilizer for soil application for 3 years, in comparison with manure and chemical fertilizer. The results of the industrial-scale treatment and 3-year field application are useful for a risk assessment of EFR and for related policymaking.

2. Material and methods

2.1. Industrial-scale treatment of erythromycin fermentation residue

EFR is the byproduct of the erythromycin production process; it contains mainly inactive mycelial dregs, fermentation medium, erythromycin, and metabolites. In this study, we investigated the industrial-scale treatment of EFR during 2018 to 2020 at a pharmaceutical facility in the Xinjiang Uygur Autonomous Region, China, which intended to produce treated EFR as a soil organic amendment. The annual handling capacity of the facility is 100 000 tonnes of EFR. The steps in the industrial-scale treatment of the fermentation residue include hydrothermal treatment (160 °C, over 15 min) and spray drying (450 °C, over 5 s). Although 160 °C is the optimum temperature, the actual operating temperature ranged from 130 to 170 °C. In 2020, a thermal insulation tank was installed after the hydrothermal treatment process in order to extend the duration of the high-temperature treatment. In the spray-drying step, a temperature of 450 °C was maintained for at least 5 s, while the entire heating and cooling process lasted for at least 20 min.

The DNA of raw EFR and of EFR just after hydrothermal treatment were extracted and visualized on agarose gels to evaluate the reduction in the genetic material present, in order to verify whether living microorganisms could survive in treated EFR. To further assess the potential remaining amounts of bacterial DNA, polymerase chain reaction (PCR) was used in an attempt to amplify the bacterial 16S ribosomal RNA (rRNA) gene.

2.2. Three-year soil application of treated EFR

Consecutive field applications of the treated EFR were performed for a 3-year period (2018–2020) in a previously undis-

turbed field located in the Xinjiang Uygur Autonomous Region, China. Soybeans were planted because the antibiotic-producing factory uses them as a fermentation medium for antibiotic production. The actual agricultural dosage and a higher dosage were respectively applied to different plots. More specifically, the land application experiment included three treatments in 2018: the control (CK; without amendment), EFR_L (low dosage, 3750 kg·hm^{-2} of treated EFR), and EFR_H (high dosage, 7500 kg·hm^{-2} of treated EFR) (Fig. S1 in Appendix A). In 2019, the dosage of treated EFR was doubled (EFR_L, 7500 of kg·hm^{-2} treated EFR; EFR_H, 15 000 kg·hm^{-2} of treated EFR) in order to investigate both the actual agricultural dosage and an extremely high dosage. Manure-derived fertilizer and chemical fertilizer were added as a comparison to the treated EFR (Fig. S1 and Section S1 in Appendix A), because they have been reported to have an influence on soil ARGs [23]. In 2020, the experimental scheme was the same as that in 2019. Considering the complexity of the field study, we used the erythromycin concentration in the soil—instead of the treated EFR dosage—as the selection pressure level, ensure that the data from different years were comparable.

Soil samples were collected with three replicates at three soybean growth stages: before each application, after each application (about 2 weeks after application), and at harvest (about 3 months after application) for 3 years. Each soil sample was divided into two parts, one of which was transferred to the laboratory on ice and stored at –20 °C for DNA extraction and erythromycin analysis, while the other was air dried and sieved (2 mm) for other chemical characterization. In total, 27 samples (3 stages × 3 treatments × 3 replicates) in 2018 and before the application of 2019; 36 samples (2 stages × 6 treatments × 3 replicates) after the application stage and harvest stage of 2019; and 54 samples (3 stages × 6 treatments × 3 replicates) in 2020 were pretreated for further chemical characterization, DNA extraction, and sequencing. More details can be found in Section S1.

2.3. Analytical methods

An elemental analyzer (Vario MAX cube, Elementar, Germany) was used to determine the total carbon (TC) and total nitrogen (TN) content of the treated EFR and soil samples. For erythromycin A measurement, solid phase extraction (SPE) procedures were performed by an Oasis HLB (6 mL per 500 mg; Waters, USA) [24]. Ultra performance liquid chromatograph-tandem mass spectroscopy (UPLC-MS/MS; Waters) was used to determine erythromycin A concentration using an Acquity UPLC BEH Shield RP18 column (1.7 μm, 2.1 mm × 100 mm; Waters) and a Waters Micromass XEVO TQ MS. More details can be found in Appendix A.

2.4. DNA extraction and 16S rRNA gene amplicon sequencing of soils

DNA extraction of the soils was performed using the FastDNA SPIN Kit (MP Biomedicals, USA) according to the manufacturer's instructions, and DNA concentration and purity were measured using NanoDrop1000 spectrophotometer (ThermoFisher, USA). The V4–V5 region of the bacterial 16S rRNA gene was amplified using PCR with the primers 515F (5'-GTGCCAGCMGCCGCGG-3') and 907R (5'-CCGTCAATTCMTTTRAGTTT-3') [25]. High-throughput sequencing was conducted on an Illumina NovaSeq PE250 platform at Guangdong Magigene Biotechnology Co. Ltd., China. The sequencing data were deposited in the National Center for Biotechnology Information (NCBI) BioProject database with the accession number PRJNA650302. More details on the 16S rRNA gene amplicon sequencing can be found in the Section S1.

2.5. Metagenomic sequencing for ARG and mobile genetic elements (MGE) quantification

Metagenomic sequencing was performed on an Illumina X-ten platform with paired-end 2 × 150 base read lengths at Guangdong Magigene Biotechnology Co., Ltd., China. Over 12 Gb of raw reads were obtained for each sample and were deposited in the NCBI BioProject database with the accession number PRJNA647129. After quality control following a previously published method [26], the filtered reads were used as inputs to ARGs-OAP v2.2, a pipeline for the characterization and quantification of ARGs from metagenomic datasets [27]. The relative abundance of the ARGs expressed as the number of copies per cell was calculated by normalizing the ARG abundance to the cell number [27], which is typical practice for normalizing gene copies in metagenomic data [28]. The "cell number" was obtained using the CopyRighter database [29,30]. A custom MGE database that collects MGE sequences from the NCBI nucleotide database and the PlasmidFinder database [31] was used to quantify the abundance of MGEs expressed as the number of copies per cell using Salmon software with the default parameters [32]. More details on the MGE database can be found in Section S1.

2.6. Metagenomic assembly and binning

Metagenomic assembly was performed for filtered reads from the samples taken after the application stage and the harvest stage in 2020 using MEGAHIT with default *k*-mer [33]. Each sample was assembled individually to obtain the contigs from each sample; these samples were then pooled and assembled together for binning. The binning of the assembled metagenomic sequencing was executed using the metaWRAP pipeline [34] with MaxBin2 for bin files [35] and Quant_bins module for the abundance of each bin in each sample. High-quality genome bins (genome quality = completeness – 5 × contamination > 50%) [36] were chosen for taxonomy assignments via the Genome Taxonomy Database (GTDB)-Tk software [37] and for ARG and MGE annotation via the Comprehensive Antibiotic Resistance Database (CARD's) Resistance Gene Identifier (RGI) software [38] and Prokka software [39]. The bins were reconstructed microbial genomes obtained from metagenomic sequencing reads and provided a possibility to link ARGs to specific hosts [40], although simple correlation analyses between ARGs and bacterial taxa are notoriously uncertain [41]. Still, when assembling genomes with highly mobile genes (e.g., many ARGs), metagenomics assembly also becomes uncertain.

2.7. Statistical analysis

Differences in nonparametric grouped data were analyzed using the Mann–Whitney *U* test or Kruskal–Wallis one-way analysis of variance (ANOVA). Principal coordinate analysis (PCoA), together with permutational multivariate analysis of variance (PERMANOVA), was used to investigate differences in the Bray–Curtis similarity of the ARGs, MGEs, and bacterial community between samples [42]. Enriched ARG subtypes in the treated EFR amendment samples taken in 2020 were obtained by means of linear discriminant analysis effect size (LEfSe) analysis [43]. For correlation analysis, the Spearman correlation was used between the abundance of ARGs and MGEs, while the Mantel test and Procrustes test were used between the ARGs and the bacterial community [44,45]. Structural equation models (SEMs) were constructed to evaluate the direct and indirect effects of erythromycin concentration, the bacterial community, and MGEs on ARGs using AMOS 22 with a robust maximum-likelihood evaluation [46]. The models were required to meet multiple goodness-of-fit criteria, including a non-significant χ^2 test ($P > 0.05$), goodness-of-fit index (GFI) > 0.90, and root mean square error of approximation (RMSEA) < 0.08 [47].

3. Results

3.1. Erythromycin concentration in industrial-scale treated EFR and field soils

The industrial-scale treatment process for EFR included hydrothermal treatment and spray drying to remove erythromycin and decrease water content prior to the EFR's land application as organic fertilizer (more details can be found in Section 2). From 2018 to 2020, the erythromycin concentration was (1659 ± 202) mg·kg^{-1} dry weight in the raw EFR. This decreased significantly after the treatment process ((350 ± 12) mg·kg^{-1} dry weight in 2018, (320 ± 26) mg·kg^{-1} dry weight in 2019, and (38 ± 1) mg·kg^{-1} dry weight in 2020). The removal of erythromycin in 2020 reached 97.7%, because the duration of the high-temperature treatment in 2020 was extended by adding thermal insulation. DNA could not be detected in the hydrothermally treated EFR by means of visualization on agarose gel (Fig. S2 in Appendix A). Attempts to amplify the bacterial 16S rRNA gene from the treated EFR via PCR also failed. Thus, the treatment greatly reduced the DNA content to non-detectable levels.

The treated EFR was used as organic fertilizer for soil applications from 2018 to 2020, while manure-derived fertilizer and chemical fertilizer were added for a comparison with the treated EFR (Fig S1). Compared with the soils that were given manure-derived fertilizer, the soils receiving treated EFR showed a much higher TN and somewhat elevated carbon content after amendment for 3 years (Tables S1 and S2 in Appendix A). Erythromycin was detected in the soils receiving treated EFR, at concentrations ranging from 0.83–76.00 μg·kg^{-1} (Fig. 1 and Table S3 in Appendix A). Overall, the erythromycin concentrations in the soils receiving low doses of treated EFR were lower than those in the soils receiving high doses of treated EFR. Across the 3 years, the erythromycin concentrations in the soils fluctuated between the application stage, the harvest stage, and the pre-application stage in the next year, but there was no obvious trend of accumulation. Erythromycin at the μg·kg^{-1} level was present in the soils receiving treated EFR before application in 2019 and 2020, indicating the expected minimal exposure during 3 years. Erythromycin was not detectable in the control soils or in the soils receiving manure fertilizer or chemical fertilizer, for which it was under the detection limit of 0.1 μg·kg^{-1} (Table S3).

3.2. Gradual shifts of soil ARGs during 3-year treated EFR application

Metagenomic sequencing was performed to quantify the abundance of ARGs in the soils receiving treated EFR or other fertilizers. The relative abundance of total ARG in the soils receiving two dosages of treated EFR was stable and did not significantly differ from the control CK in 2018 and 2019 (values ranged from 0.103 copies per cell to 0.123 copies per cell; $P > 0.05$, Kruskal–Wallis one-way ANOVA). However, after the application stage in 2020, the ARG abundance in soils receiving 7500 kg·hm^{-2} of treated EFR ((0.187 ± 0.051) copies per cell) and 15 000 kg·hm^{-2} of treated EFR ((0.278 ± 0.123) copies per cell) was significantly higher than that in the CK samples ((0.101 ± 0.003) copies per cell) (Fig. 2(a) and Table S4 in Appendix A; $P < 0.01$, Kruskal–Wallis one-way ANOVA). Although manure fertilizer and chemical fertilizer amendments increased the soil ARG abundance, the impact of the treated EFR was greater than that of the others (Fig. 2(a) and Table S4).

To clarify which ARG subtypes became enriched in the soils receiving treated EFR compared with the controls in 2020, a LEfSe analysis was performed. The results showed that seven genes (*erm* (39), *erm*B, *erm*F, *erm*T, *mac*B, *mgt*A, and *ole*D) belonging to the family of macrolide–lincosamide-streptogramin (MLS) resistance genes and 20 genes belonging to other types of ARGs were enriched in the treated-EFR-amended soils in 2020 (Fig. 2(b)). The resistance genes *erm*T, *erm*B and *mac*B (average abundance of 0.055 copies per cell, 0.009 copies per cell and 0.005 copies per cell, respectively, in the high-dosage treatment group) were the most abundant MLS resistance genes after treated EFR application in 2020 (Tables S5–S7 in Appendix A). In the samples of after application stage in 2020, the enrichments of total ARGs and MLS resistance genes were significant (Fig. 2). Notably, the fold change of MLS resistance genes in the high-dosage treated-EFR-application soil was 12.59 times compared with that in the CK, while the fold change of the total ARGs was only 2.75 times. This finding indicated the selective enrichment of MLS resistance genes.

The changes in ARG structure showed a similar trend as the ARG abundance over the 3 years. ARG β diversity was plotted using PCoA, with further PERMANOVA to examine the influence of sampling stage and treatment (Fig. 3(a)). In 2018 and 2019, the ARG structure was distinct between the three sampling stages ($P < 0.01$, PERMANOVA), but amendment with treated EFR led to a negligible impact ($P > 0.05$, PERMANOVA). However, in 2020,

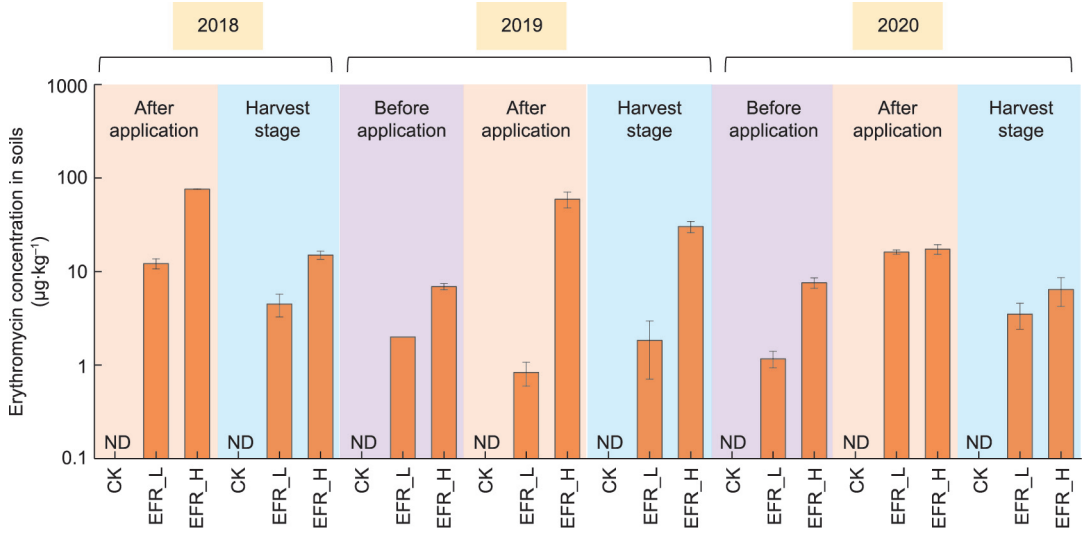

Fig. 1. Erythromycin concentration in soils receiving treated EFR during 3-year (2018, 2019, and 2020) field application. ND: not detected; EFR_L: soils receiving 3750 kg·hm^{-2} of treated EFR in 2018 or 7500 kg·hm^{-2} of treated EFR in 2019 and 2020; EFR_H: soils receiving 7500 kg·hm^{-2} of treated EFR in 2018, or 15 000 kg·hm^{-2} of treated EFR in 2019 and 2020.

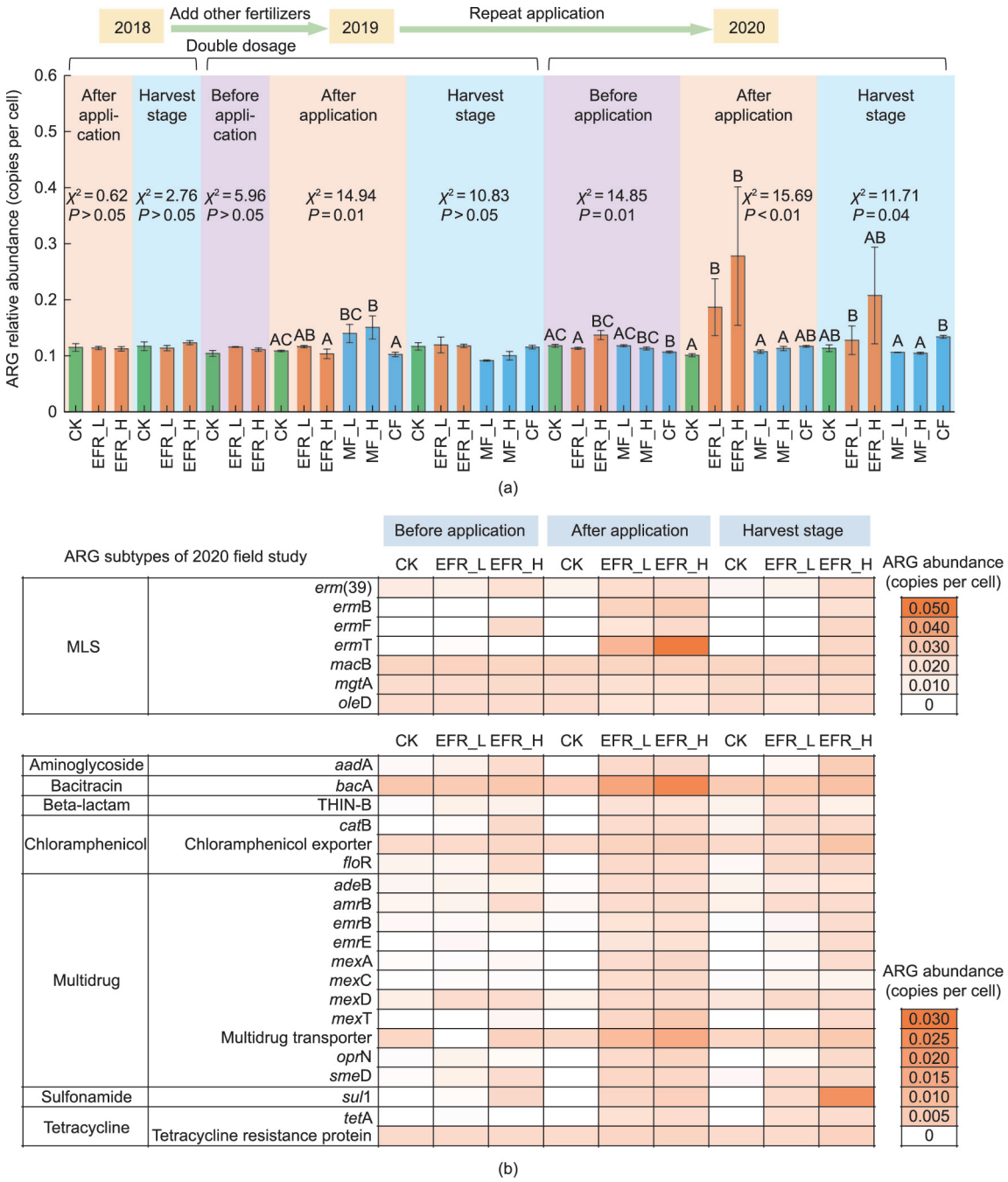

Fig. 2. ARG abundance in soils receiving treated EFR, manure-derived fertilizer, and chemical fertilizer in three sampling stages (before application, after application, and harvest stage) for 3 years (2018, 2019, and 2020). (a) Total abundance of detected ARGs. Samples within one stage were compared and labeled with the same letter if not significantly different from each other based on Kruskal-Wallis one-way ANOVA. (b) Abundance of ARG subtypes of soils in 2020. Only subtypes enriched in the treated-EFR-amended soils according to LEfSe analysis are shown. MF_L and MF_H: soils receiving 7500 and 15 000 kg·hm^{-2} of manure-derived fertilizer, respectively; CF: soils receiving chemical fertilizer.

the ARG structure of the treated-EFR-amended soils exhibited clear differences with that of the CK soils (Fig. 2(a); $P < 0.05$, PERMANOVA). In addition, to obtain detailed information on the ARG structure at each stage of each year, the Bray–Curtis similarities within CK and between CK and the treated groups were compared. At the harvest stage in 2019, before the application stage in 2020, and after the application stage in 2020, the treated EFR amendment decreased the ARG similarity compared with the CK (Fig. 3 (b); $P < 0.05$, Mann–Whitney U test).

In summary, within the experimental period of 3 years, the treated EFR was used as organic fertilizer; however, its impact on the soil ARGs was not immediately detectable. It was not until the second and third years (i.e., the harvest stage of 2019 and all sampling times in 2020) that the ARG abundance and diversity clearly diverged between the amended and control treatments.

3.3. Dynamics of the soil bacterial community and MGEs during the 3 years of treated EFR application

The abundance and structure of the soil bacterial community and MGEs during the 3-year experiment were assessed. At the phylum level, *Actinobacteria*, *Bacteroidetes*, *Firmicutes*, and

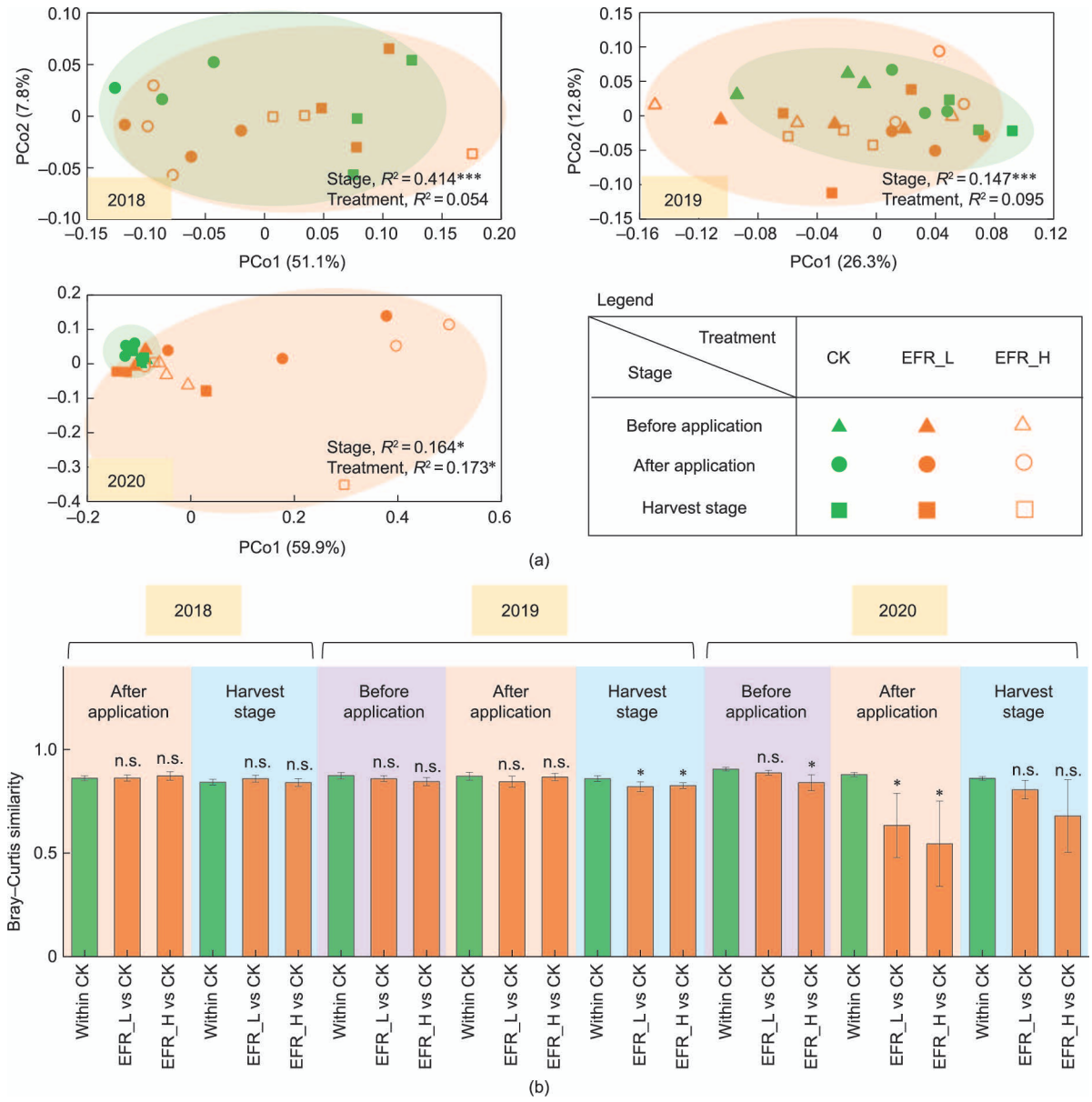

Fig. 3. ARG structure in soils receiving treated EFR in three sampling stages (before application, after application, and harvest stage) for 3 years (2018, 2019, and 2020). (a) PCoA and PERMANOVA of ARGs in three sampling stages for three years. (b) Bray–Curtis similarity of ARGs within CK soils and between CK soils and soils receiving treated EFR. Samples were compared with "within CK" based on Mann–Whitney *U* tests. n.s., *, **, and *** indicate $P \geq 0.05$, < 0.05, < 0.01, and < 0.001, respectively.

Proteobacteria were the main bacterial phyla detected in the soils (Fig. S3, Tables S8–S10 in Appendix A). The bacterial community structure was only influenced by the sampling stage in 2018, but was influenced by both the sampling stage and the treated EFR application in 2019 and 2020 (Fig. S4(a) in Appendix A). The Bray–Curtis similarity between the control and amended groups became significantly different after the harvest stage in 2018. These results indicated that the shift in the bacterial community occurred earlier in the experiment than the shift in ARGs did.

MGEs are associated with the horizontal transfer of ARGs and mainly consist of integrons, transposons, and plasmid and insertion sequences (details can be found in the Section S1). In 2018 and 2019, the MGE abundances of the CK soils and the treated-EFR-amended soils were similar (ranging from 0.003 copies per cell to 0.009 copies per cell; $P > 0.05$, Kruskal–Wallis one-way ANOVA). However, in 2020, the MGE abundance in the soils receiving treated EFR became higher than that in the CK soils. The highest MGE abundance was 0.042 copies per cell in the soils receiving 15 000 kg·hm^{-2} of treated EFR at the harvest stage in 2020 (Fig. S5(a) and Table S11 in Appendix A). The most abundant MGE was *tnpA*, followed by IS*91* and *intI*1 (Fig. S5(b), Tables S12–S14). Similar to the ARG structure, the MGE structure was only influenced by the sampling stage in 2018 and 2019, but was influenced by both the sampling stage and the treated EFR amendment in 2020, as revealed by the PCoA and PERMANOVA results (Fig. S6 in Appendix A).

3.4. Contribution of MGEs, the bacterial community, and erythromycin to ARG dynamics

Correlations between ARG abundance and MGE abundance were not statistically significant in 2018 (Spearman's r = –0.11, $P > 0.05$) or 2019 (Spearman's r = 0.29, $P > 0.05$) but were significant in 2020 (Spearman's r = 0.73, $P < 0.01$) (Fig. 4(a)). Some MLS resistance genes (*erm*(39), *erm*B, *erm*F, and *erm*T) showed widespread association with MGE types ($P < 0.05$, Spearman

correlation); however, correlations between *mac*B, *mgt*A, and *ole*D, and MGEs were not significant (Fig. 4(b)). Links between the bacterial community and ARGs were quantified using the Mantel test and Procrustes test. Although the statistical differences were significant in all 3 years, the correlation coefficient (*r* value) became higher from 2018 to 2020 (*r* = 0.611, 0.618, and 0.894 in 2018, 2019, and 2020, respectively, Mantel test; *r* = 0.737, 0.729, and 0.922 in 2018, 2019, and 2020, respectively, Procrustes test) (Fig. 4(c)).

To obtain a holistic understanding of the contribution of MGEs, the bacterial community, and erythromycin to ARG dynamics, SEMs among these variables were conducted. Erythromycin affected ARGs by influencing the bacterial community and MGEs in 2020. ARGs were restricted only by the bacterial community in 2018, but were restricted by both the bacterial community and MGEs in 2019 and 2020 (Fig. 4(d)). Overall, MGEs, the bacterial community, and erythromycin showed an increasing contribution to ARG dynamics during the 3-year consecutive field applications of treated EFR, and the explanation ratio of the ARGs increased from 67.5% in 2018 to 95.6% in 2020 (Fig. 4(d)).

3.5. Enrichment of putative ARG-carrying hosts revealed by metagenomic binning

Metagenomic assembly and binning was used to explore ARG-carrying contigs and putative ARG-carrying bacterial hosts, in order to determine the genetic environment of the ARGs and the relative abundance of ARG-carrying bins in different samples. From the metagenomic results for the after application stage and the harvest stage samples in 2020, 68 ARG-carrying contigs were found, among which 10 contigs carried MLS resistance genes (*erm*B, *erm*T, *mac*A, and *mac*B). Representative MLS resistance gene-carrying contigs are shown in Fig. 5(a). A Tn*3* family transposase—a typical MGE—was linked to *erm* genes. The resistance genes *mac*A and *mac*B and an adenosine triphosphate (ATP)-binding cassette (ABC) transporter co-occurred on one contig (Fig. 5(a)). Notably, contigs that carried MLS resistance genes could not be recovered from the control samples, indicating that only predominant genes could be obtained in contigs via the metagenomic assembly.

Using the metagenomic binning approach, 12 bins were identified as high-quality metagenome-assembled genomes (completeness – 5 × contamination > 50%), and their taxonomies were identified via GTDB-Tk software. They were assigned to Verrucomicrobia, Proteobacteria, Bacteroidota, and Actinobacteriota in the GTDB-Tk software (Fig. 5(b), Tables S15 and S16 in Appendix A). Therein, eight bins carried MLS resistance genes (*mac*A, *mac*B, or *ole*D), and their relative abundance in the soils amended with treated EFR was higher than that in the controls. In contrast, the relative abundances of bins without MLS genes (e.g., bin.479 and bin.62) were stable or lower in the soils receiving treated EFR compared with the controls (Fig. 5(b) and Tables S15). In addition, the enrichment of the MLS resistance gene-carrying bins led to the enrichment of co-occurring genes such as *tet*A (Figs. 2(b) and 5(b)).

4. Discussion

Hydrothermal treatment of EFR kills microorganisms and degrades their DNA. Consequently, residual antibiotic is the main risk factor in the recycling of treated antibiotic fermentation

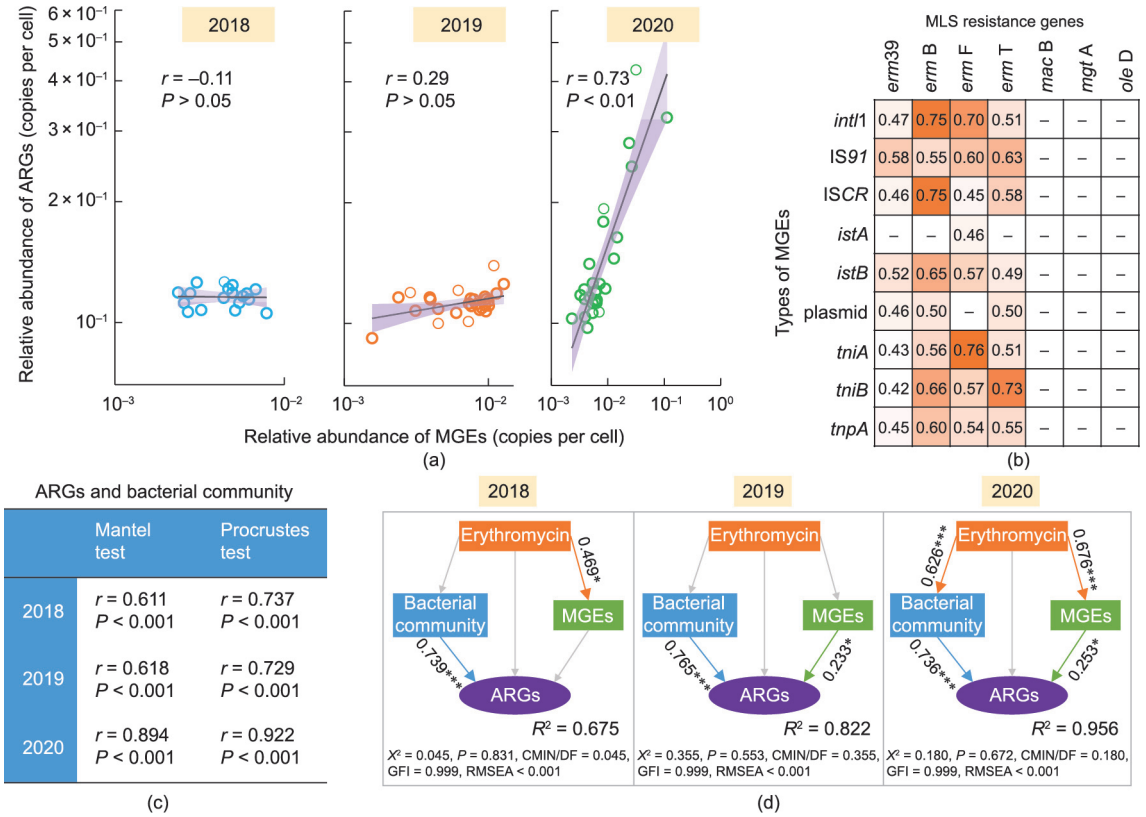

Fig. 4. ARG variation to MGEs, bacterial community, and erythromycin of soils during 3 years of EFR application. (a) Spearman correlation between relative abundance of ARGs and relative abundance of MGEs during the 3-year (2018, 2019, and 2020) field study. (b) Spearman correlation between dominant MLS resistance genes and types of MGEs in the 2020 field study. Only the correlation coefficients (*r* values) of significant results ($P < 0.05$) are shown. (c) Mantel test and Procrustes test between ARGs and the bacterial community of soils. (d) Contribution of erythromycin, the bacterial community and MGEs to soil ARG variation during the 3-year (2018, 2019, and 2020) field study, as revealed by the SEM.

residue as a soil amendment. The extent to which residual erythromycin from EFR would promote the proliferation and spread of antibiotic resistance in soils is then the key issue in the safe disposal and environmental management of EFR. Here, we performed, to the best of our knowledge, the first study on the use of industrial-scale treated EFR as a soil amendment for multiyear land application.

The sustained input of the treated EFR led to relatively stable sub-inhibitory levels of erythromycin in the soil. As a result of the study design, we were able to investigate the long-term impact of treated EFR soil amendment and understand the underlying mechanism of antibiotic resistome development induced by sub-inhibitory antibiotics.

4.1. Accumulated effect of treated EFR on soil ARGs during the 3-year period

The soil erythromycin concentration decreased after the application of EFR compared with the concentrations at the time of harvest and prior to the next year's addition (Fig. 1). The transformation processes of erythromycin in the environment, which include adsorption, hydrolytic cleavage, microbial degradation, and photochemical degradation, have been verified [48]. Thus, surface run-off, infiltration, hydrolysis, and biodegradation may have contributed to the loss of erythromycin [17]. However, the limited loss resulted in maintained $\mu g \cdot kg^{-1}$ concentrations of erythromycin in the soils for the 3 years of application [19]. Soil ARGs and relevant determinants (MGEs and the bacterial community) were characterized across the 3 years by means of high-throughput sequencing. The response of these biotic variables to erythromycin addition appeared to require some time to develop.

The bacterial community structure had changed by the harvest stage of the first year (2018), but the ARGs and MGEs did not change in a detectable way until the second (2019) and third (2020) years, respectively (Fig. 2, Fig. 3, and Tables S3–S6). Notably, although the erythromycin concentrations in the treated EFR and in the soils amended with the treated EFR in 2018 or 2019 were higher than those in 2020 (Fig. 1(b)), the ARG abundance did not increase significantly in 2018 or 2019, but clearly increased in 2020 (Fig. 2). Such gradual changes of the ARGs indicate that there

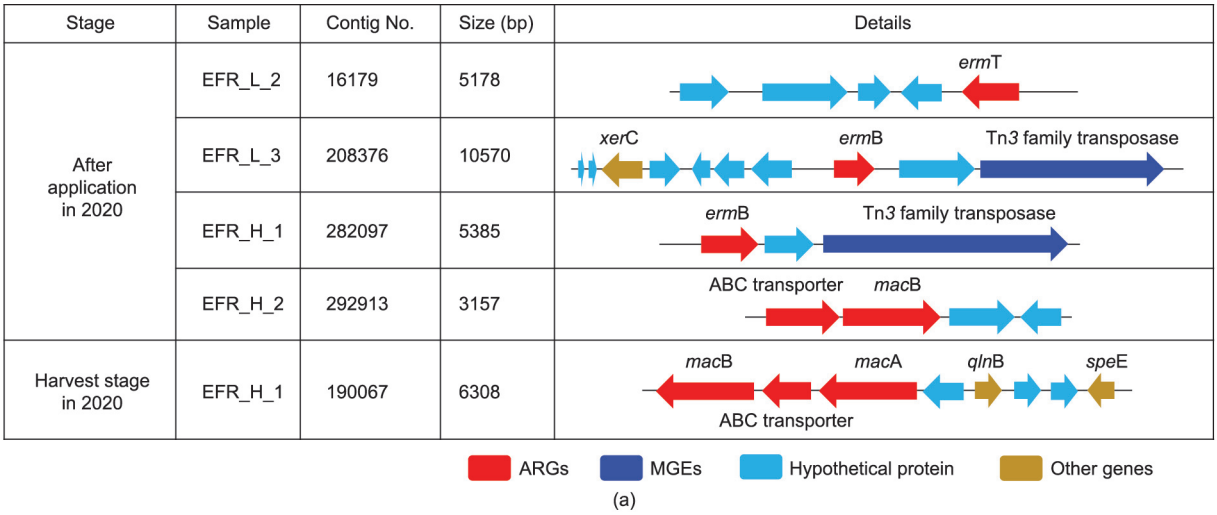

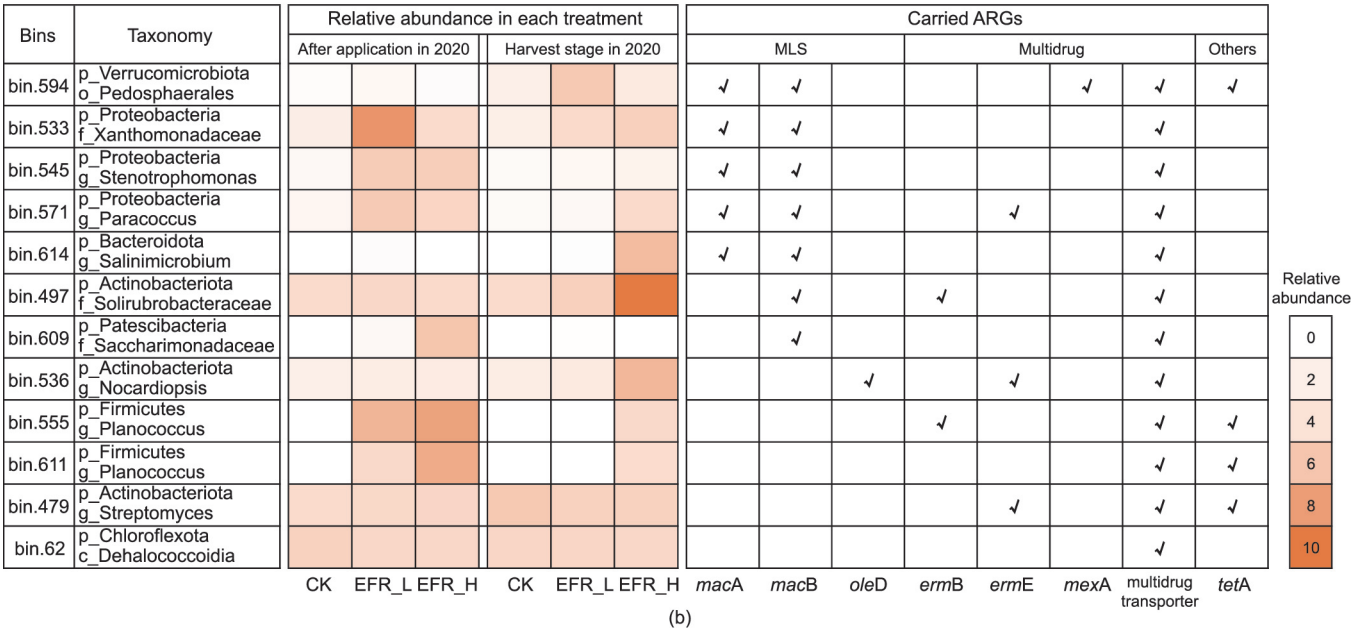

Fig. 5. (a) Representative ARG-carrying metagenome-assembled contigs and (b) GTDB taxonomy, relative abundance, and ARG distribution of metagenome-assembled genomes obtained by the metagenomic binning approach from soil metagenomic sequencing data of the after application stage and harvest stage in 2020. Only high-quality metagenome-assembled genomes (completeness – 5 × contamination > 50%) are shown.

is a cumulative impact of long-term exposure to sub-inhibitory concentrations of erythromycin via treated EFR, which is not revealed by a single-year application experiment. In addition, no cumulative effect on the total abundance of soil ARGs was found after the 2-year application of manure-derived fertilizer; a plausible explanation is that most manure-derived bacteria may not persist in the soil environment [49]. In this study, the specific enrichment of macrolide-ARGs was greater than that of other ARGs. This finding supported direct selection pressure by erythromycin, rather than the indirect effect of introduced nutrients, as the latter would not specifically enrich macrolide-ARGs over other ARGs. Such persistent selection pressure on diverse microbial ecosystems, such as soils, may result in risks promoting the evolution (mobilization and horizontal transfer) of yet-undiscovered forms of macrolide resistance and may eventually pose additional challenges in the clinic [3,50].

4.2. Potential mechanisms of soil ARG enrichment under sub-inhibitory erythromycin concentrations

To disentangle the mechanism of ARG enrichment under sub-inhibitory erythromycin concentrations, metagenomic sequencing, bioinformatic analyses, and multivariate statistics were used. The long-term impact of erythromycin exposure has been assessed using *msr*E and *mph*E genes as markers [17,18]. Here, we attempted to screen for all known ARGs and reveal the contribution of vertical and horizontal pathways to ARG proliferation.

Within the enriched MLS genes, *erm*B, *erm*F, and *erm*T were dominant (Fig. 2(b), Tables S4–S7). These *erm* genes showed a significant correlation with diverse types of MGEs (Fig. 4(b)) and co-occurred with Tn*3* family transposase, a typical MGE, in a contig from the metagenomic assembly (Fig. 5(a)). The *erm* genes were not found in the bacterial genomes assembled from the metagenomic data (Fig. 5(b)). Also, because binning approaches tend to be unable to reconstruct plasmids [41], these results hinted that the *erm* genes were carried by plasmids and accumulated via horizontal gene transfer under erythromycin selection pressure. The key role of horizontal gene transfer on the dissemination of *erm* genes is supported by previous work. Most *erm* genes were first described from plasmids; for example, *erm*T was found in pGT633 [51,52] and p121BS [53], and was flanked by IS*1216V* [54]. Recently, bacterial conjugation efficiency was found to be significantly promoted by macrolides [55], which further supports the potential enrichment of MGEs and plasmid-carrying ARGs in this experiment.

The efflux pump genes *mac*A and *mac*B confer resistance against macrolides composed of 14-membered (e.g., erythromycin) and 15-membered lactones [56,57]. In contrast to *erm* genes, the *mac*A and *mac*B in this study exhibited weak links with MGEs according to the correlation analysis (Fig. 4(b)) and metagenomic assembly (Fig. 5(a)), and commonly occurred on the bacterial genomes assembled from the metagenomic sequences (Fig. 5(b)). All these results suggest that *mac*A and *mac*B tend to be located on bacterial chromosomes, and that the enrichment of *mac* gene-carrying bacterial hosts under erythromycin pressure contributed to the enriched abundance of *mac* genes.

Some ARGs that did not confer MLS resistance also became enriched (Fig. 2(b)). A plausible explanation for this phenomenon is the co-selection of MLS genes and other genes. For example, *tet*A, *mac*A, and *mac*B co-occurred in bin.594, and the enrichment of this bin resulted in the increased abundance of both *mac* genes and *tet*A (Fig. 5(b)). According to the multivariate statistical results, within the 3-year period, the links between ARGs and the bacterial community (the vertical pathway) and MGEs (the horizontal pathway) became gradually stronger (Figs. 4(a) and (c)), and the SEM results further confirmed this trend (Fig. 4(d)).

Because sub-inhibitory concentrations of antibiotics do not kill sensitive bacteria but may simply decrease their growth rate [20,58,59], such concentrations could still give resistant bacteria a competitive edge, resulting in the enrichment of ARGs. In addition, sub-inhibitory antibiotic concentrations could induce the SOS response and the RpoS regulon, both of which are known to enhance the rates of horizontal gene transfer and thereby increase the abundance of ARGs [20].

In sum, the combined effects of horizontal and vertical pathways led to a bloom of ARGs under the sub-inhibitory concentrations of erythromycin in the soils receiving treated EFR over 3 years. At the harvest stage in 2020, the ARG abundance was lower than after application stage. A plausible explanation is that the fitness costs of plasmid carriage imposed negative impacts on the reproduction and survival of bacteria [60]. A different indigenous bacterial community might lead to different ARG variation under selection pressure, and diverse kinds of agricultural soils may respond differently [61]. Further research on the impact of EFR should take soil type into account.

4.3. Environmental and engineering implications

Soil amendment is commonly mixed with soil once or several times per year. Thus, multiyear monitoring and time-series sampling are vital for the assessment of soil amendments. In this study, the degradation of erythromycin in soils was relatively slow compared with the degradation of some other antibiotics, such as streptomycin [9], causing the "entrance-dissipation" dynamic of erythromycin during the 3 years. The presence of $\mu g \cdot kg^{-1}$ levels of erythromycin persisted for 3 years, and the ARG structure and ARG abundance began to change in a detectable way in the second and the third years. Our results emphasize that application frequency is an important variable for evaluating the environmental impact of treated EFR soil amendment. In addition, other kinds of antibiotic fermentation residue, manure fertilizer [62], activated sludge [63], and reclaimed water [64] have been added to soils, and all of these contain antibiotics. Based on our results, we urgently call for prudent examination of the long-term impact of sub-inhibitory antibiotics from the abovementioned sources. For practical reasons, our study had limited replication of soil plots; thus, a more intricate randomized plot design could be valuable in future evaluation studies [65].

In agricultural practice, the amount of TN from organic manure should not exceed 250 $kg \cdot hm^{-2}$ within 1 year at the field level [66], and the TN content of the treated EFR was around 50 $g \cdot kg^{-1}$. Thus, in this study, the high-dosage application of treated EFR tended to be a very high dosage (375–750 kg of TN per hectare per year). The actual agricultural need might be closer to the low-dosage application adopted in the present study, which showed limited antibiotic resistance development compared with the high-dosage application within the 3-year experiment period. The long-term application of treated EFR at a different dosage was vital for its risk management [65].

We cannot exclude the possibility that the lower dosages given in the first year could have played a role in the absence of discernable effects on the resistome. Whether the multiyear soil application of treated EFR with a lower concentration of remaining erythromycin than that in this study would affect the soil resistome, and whether the use of treated EFR in alternate years would mitigate its environmental impact, needs further exploration.

The utilization of antibiotic fermentation residue as a soil amendment is beneficial for a circular economy and for carbon-neutrality [67], but the risks such practices may bring must also be considered carefully. Heat treatment effectively removed the risks associated with the spread of resistant microorganisms, which was potentially promoted during the fermentation process.

The heat treatment also led to the effective removal of the genetic material of such organisms. The key remaining objective of engineering operations to recycle antibiotic fermentation residue is to remove residual antibiotics, and thus prevent environmental contamination from these biologically active agents. Here, industrial-scale hydrothermal treatment was used to remove erythromycin from EFR. It also enhanced the release of protein-like polymers for better utilization of the EFR as a fertilizer or bioenergy [14]. The efficacy of erythromycin removal was improved by extending the high-temperature treatment time. More effective and economical methods, such as hydrothermal treatment with solid base catalysts [68] and hydrothermal carbonization [69], are potential options for better antibiotic removal.

5. Conclusions

An important—though not always emphasized—source of environmental antibiotic pollution is fermentation residue, a byproduct of the antibiotic pharmaceutical industry. This study performed a multiyear survey of industrial-scale EFR treatment and the *in situ* land application of treated EFR. The removal ratio of erythromycin from EFR was as high as 97.7%, and consecutive treated EFR applications maintained sub-inhibitory ($\mu g \cdot kg^{-1}$ level) erythromycin concentrations in the soils for the 3 years of the study. The land application of a high dosage of treated EFR showed an accumulated impact on soil ARGs based on time-series sampling, and the impact of an actual agricultural dosage was weaker than that of a high dosage. In addition, systematic data mining of metagenomic sequences showed that horizontal and vertical dissemination pathways were involved in the increased abundance of *erm* genes and *mac* genes, respectively. These findings are useful for the risk assessment and environmental management of antibiotic fermentation residue and other wastes containing antibiotics.

Acknowledgment

Financial support for this study was obtained from National Natural Science Foundation of China (32141002 and 22076203). We thank Mr. Zhijie Li for help in sampling.

Compliance with ethics guidelines

Ziming Han, Haodi Feng, Xiao Luan, Yunpeng Shen, Liren Ren, Liujie Deng, D.G. Joakim Larsson, Michael Gillings, Yu Zhang, and Min Yang declare that they have no conflict of interest or financial conflicts to disclose.

Appendix A. Supplementary data

Supplementary data to this article can be found online at https://doi.org/10.1016/j.eng.2022.05.011.

References

[1] Larsson DGJ. Pollution from drug manufacturing: review and perspectives. Philos Trans R Soc Lond B Biol Sci 2014;369(1656):20130571.
[2] Berendonk TU, Manaia CM, Merlin C, Fatta-Kassinos D, Cytryn E, Walsh F, et al. Tackling antibiotic resistance: the environmental framework. Nat Rev Microbiol 2015;13(5):310–7.
[3] Larsson DGJ, Flach CF. Antibiotic resistance in the environment. Nat Rev Microbiol 2022;20(5):257–69.
[4] Bewick MWM. Use of antibiotic fermentation wastes as fertilizers for tomatoes. J Agric Sci 1979;92(3):669–74.
[5] Zhang Q, Ying G, Pan C, Liu Y, Zhao J. Comprehensive evaluation of antibiotics emission and fate in the river basins of China: source analysis, multimedia modeling, and linkage to bacterial resistance. Environ Sci Technol 2015;49(11):6772–82.
[6] Ding Y, Zhang W, Gu C, Xagoraraki I, Li H. Determination of pharmaceuticals in biosolids using accelerated solvent extraction and liquid chromatography/tandem mass spectrometry. J Chromatogr A 2011;1218(1):10–6.
[7] Carvalho RN, Ceriani L, Ippolito A, Lettieri T. Development of the 1st Watch List under the Environmental Quality Standards Directive. Report. Luxembourg: Publications Office of the European Union. 2015. Report No.: EUR 27142 EN.
[8] Bengtsson-Palme J, Larsson DGJ. Concentrations of antibiotics predicted to select for resistant bacteria: proposed limits for environmental regulation. Environ Int 2016;86:140–9.
[9] Tang M, Gu Y, Wei D, Tian Z, Tian Y, Yang M, et al. Enhanced hydrolysis of fermentative antibiotics in production wastewater: hydrolysis potential prediction and engineering application. Chem Eng J 2020;391:123626.
[10] He Y, Tian Z, Yi Q, Zhang Yu, Yang M. Impact of oxytetracycline on anaerobic wastewater treatment and mitigation using enhanced hydrolysis pretreatment. Water Res 2020;187:116408.
[11] Tang M, Li F, Yang M, Zhang Y. Degradation of kanamycin from production wastewater with high-concentration organic matrices by hydrothermal treatment. J Environ Sci (China) 2020;97:11–8.
[12] Yi Q, Zhang Y, Gao Y, Tian Z, Yang M. Anaerobic treatment of antibiotic production wastewater pretreated with enhanced hydrolysis: simultaneous reduction of COD and ARGs. Water Res 2017;110:211–7.
[13] Yousefifar A, Baroutian S, Farid MM, Gapes DJ, Young BR. Fundamental mechanisms and reactions in non-catalytic subcritical hydrothermal processes: a review. Water Res 2017;123:607–22.
[14] Cai C, Hua Yu, Li H, Li L, Dai L, Liu H, et al. Hydrothermal treatment of erythromycin fermentation residue: harmless performance and bioresource properties. Resour Conserv Recycling 2020;161:104952.
[15] Zhang Y, Liu H, Dai X, Cai C, Wang J, Wang M, et al. Impact of application of heat-activated persulfate oxidation treated erythromycin fermentation residue as a soil amendment: soil chemical properties and antibiotic resistance. Sci Total Environ 2020;736:139668.
[16] Luan X, Han Z, Shen Y, Yang M, Zhang Y. Assessing the effect of treated erythromycin fermentation residue on antibiotic resistome in soybean planting soil: *in situ* field study. Sci Total Environ 2021;779:146329.
[17] Topp E, Renaud J, Sumarah M, Sabourin L. Reduced persistence of the macrolide antibiotics erythromycin, clarithromycin and azithromycin in agricultural soil following several years of exposure in the field. Sci Total Environ 2016;562:136–44.
[18] Lau CHF, Tien YC, Stedtfeld RD, Topp E. Impacts of multi-year field exposure of agricultural soil to macrolide antibiotics on the abundance of antibiotic resistance genes and selected mobile genetic elements. Sci Total Environ 2020;727:138520.
[19] Chow LKM, Ghaly TM, Gillings MR. A survey of sub-inhibitory concentrations of antibiotics in the environment. J Environ Sci 2021;99:21–7.
[20] Andersson DI, Hughes D. Microbiological effects of sublethal levels of antibiotics. Nat Rev Microbiol 2014;12(7):465–78.
[21] Jørgensen KM, Wassermann T, Jensen PØ, Hengzuang W, Molin S, Høiby N, et al. Sublethal ciprofloxacin treatment leads to rapid development of high-level ciprofloxacin resistance during long-term experimental evolution of *Pseudomonas aeruginosa*. Antimicrob Agents Chemother 2013;57(9):4215–21.
[22] Andersson DI, Hughes D. Evolution of antibiotic resistance at non-lethal drug concentrations. Drug Resist Updat 2012;15(3):162–72.
[23] Xie W, Yuan S, Xu M, Yang X, Shen Q, Zhang W, et al. Long-term effects of manure and chemical fertilizers on soil antibiotic resistome. Soil Biol Biochem 2018;122:111–9.
[24] Wang Y, Li S, Zhang F, Lu Y, Yang B, Zhang F, et al. Study of matrix effects for liquid chromatography-electrospray ionization tandem mass spectrometric analysis of 4 aminoglycosides residues in milk. J Chromatogr A 2016;1437:8–14.
[25] Fouhy F, Clooney AG, Stanton C, Claesson MJ, Cotter PD. 16S rRNA gene sequencing of mock microbial populations—impact of DNA extraction method, primer choice and sequencing platform. BMC Microbiol 2016;16:123.
[26] Yan L, Yang M, Guo H, Yang L, Wu J, Li R, et al. Single-cell RNA-Seq profiling of human preimplantation embryos and embryonic stem cells. Nat Struct Mol Biol 2013;20(9):1131–9.
[27] Yin X, Jiang XT, Chai B, Li L, Yang Y, Cole JR, et al. ARGs-OAP v2.0 with an expanded SARG database and Hidden Markov Models for enhancement characterization and quantification of antibiotic resistance genes in environmental metagenomes. Bioinformatics 2018;34(13):2263–70.
[28] Ju F, Beck K, Yin X, Maccagnan A, McArdell CS, Singer HP, et al. Wastewater treatment plant resistomes are shaped by bacterial composition, genetic exchange, and upregulated expression in the effluent microbiomes. ISME J 2019;13(2):346–60.
[29] Angly FE, Dennis PG, Skarshewski A, Vanwonterghem I, Hugenholtz P, Tyson GW. CopyRighter: a rapid tool for improving the accuracy of microbial community profiles through lineage-specific gene copy number correction. Microbiome 2014;2:11.
[30] Yang Y, Jiang X, Chai B, Ma L, Li B, Zhang A, et al. ARGs-OAP: online analysis pipeline for antibiotic resistance genes detection from metagenomic data using an integrated structured ARG-database. Bioinformatics 2016;32(15):2346–51.
[31] Pärnänen K, Karkman A, Hultman J, Lyra C, Bengtsson-Palme J, Larsson DGJ, et al. Maternal gut and breast milk microbiota affect infant gut antibiotic resistome and mobile genetic elements. Nat Commun 2018;9:3891.
[32] Patro R, Duggal G, Love MI, Irizarry RA, Kingsford C. Salmon provides fast and bias-aware quantification of transcript expression. Nat Methods 2017;14(4):417–9.

[33] Li D, Liu CM, Luo R, Sadakane K, Lam TW. MEGAHIT: an ultra-fast single-node solution for large and complex metagenomics assembly via succinct de Bruijn graph. Bioinformatics 2015;31(10):1674–6.
[34] Uritskiy GV, DiRuggiero J, Taylor J. MetaWRAP—a flexible pipeline for genome-resolved metagenomic data analysis. Microbiome 2018;6:158.
[35] Wu YW, Simmons BA, Singer SW. MaxBin 2.0: an automated binning algorithm to recover genomes from multiple metagenomic datasets. Bioinformatics 2016;32(4):605–7.
[36] Parks DH, Rinke C, Chuvochina M, Chaumeil PA, Woodcroft BJ, Evans PN, et al. Recovery of nearly 8000 metagenome-assembled genomes substantially expands the tree of life. Nat Microbiol 2017;2(11):1533–42.
[37] Chaumeil PA, Mussig AJ, Hugenholtz P, Parks DH. GTDB-Tk: a toolkit to classify genomes with the Genome Taxonomy Database. Bioinformatics 2019;36:1925–7.
[38] Alcock BP, Raphenya AR, Lau TTY, Tsang KK, Bouchard M, Edalatmand A, et al. CARD 2020: antibiotic resistome surveillance with the comprehensive antibiotic resistance database. Nucleic Acids Res 2020;48(D1):D517–25.
[39] Seemann T. Prokka: rapid prokaryotic genome annotation. Bioinformatics 2014;30(14):2068–9.
[40] Yuan L, Wang Y, Zhang L, Palomo A, Zhou J, Smets BF, et al. Pathogenic and indigenous denitrifying bacteria are transcriptionally active and key multi-antibiotic-resistant players in wastewater treatment plants. Environ Sci Technol 2021;55(15):10862–74.
[41] Rice EW, Wang P, Smith AL, Stadler LB. Determining hosts of antibiotic resistance genes: a review of methodological advances. Environ Sci Technol Lett 2020;7(5):282–91.
[42] Anderson MJ. A new method for non-parametric multivariate analysis of variance. Austral Ecol 2001;26(1):32–46.
[43] Segata N, Izard J, Waldron L, Gevers D, Miropolsky L, Garrett WS, et al. Metagenomic biomarker discovery and explanation. Genome Biol 2011;12(6):R60.
[44] Peres-Neto PR, Jackson DA. How well do multivariate data sets match? The advantages of a Procrustean superimposition approach over the Mantel test. Oecologia 2001;129(2):169–78.
[45] Smouse PE, Long JC, Sokal RR. Multiple-regression and correlation extensions of the mantel test of matrix correspondence. Syst Zool 1986;35(4):627–32.
[46] Byrne BM. Structural equation modeling with amos: basic concepts, applications, and programming. Mahwah: Lawrence Erlbaum Associates Publishers; 2001.
[47] Schermelleh-Engel K, Moosbrugger H, Müller H. Evaluating the fit of structural equation models: tests of significance and descriptive goodness-of-fit measures. Methods Psychol Res Online 2003;8:23–74.
[48] Senta I, Kostanjevecki P, Krizman-Matasic I, Terzic S, Ahel M. Occurrence and behavior of macrolide antibiotics in municipal wastewater treatment: possible importance of metabolites, synthesis byproducts, and transformation products. Environ Sci Technol 2019;53(13):7463–72.
[49] Muurinen J, Stedtfeld R, Karkman A, Pärnänen K, Tiedje J, Virta M. Influence of manure application on the environmental resistome under finnish agricultural practice with restricted antibiotic use. Environ Sci Technol 2017;51(11):5989–99.
[50] Bengtsson-Palme J, Larsson DGJ. Antibiotic resistance genes in the environment: prioritizing risks. Nat Rev Microbiol 2015;13(6):396.
[51] Roberts MC, Sutcliffe J, Courvalin P, Jensen LB, Rood J, Seppala H. Nomenclature for macrolide and macrolide–lincosamide–streptogramin B resistance determinants. Antimicrob Agents Chemother 1999;43(12):2823–30.
[52] Saribas Z, Tunckanat F, Pinar A. Prevalence of erm genes encoding macrolide-lincosamide-streptogramin (MLS) resistance among clinical isolates of *Staphylococcus aureus* in a Turkish university hospital. Clin Microbiol Infect 2006;12(8):797–9.
[53] Whitehead TR, Cotta MA. Sequence analyses of a broad host-range plasmid containing *erm*T from a tylosin-resistant *Lactobacillus* sp. isolated from swine feces. Curr Microbiol 2001;43(1):17–20.
[54] Tsai JC, Hsueh PR, Chen HJ, Tseng SP, Chen PY, Teng LJ. The *erm*(T) gene is flanked by IS*1216V* in inducible erythromycin-resistant *Streptococcus gallolyticus* subsp. *pasteurianus*. Antimicrob Agents Chemother 2005;49(10):4347–50.
[55] Bethke JH, Davidovich A, Cheng L, Lopatkin AJ, Song W, Thaden JT, et al. Environmental and genetic determinants of plasmid mobility in pathogenic *Escherichia coli*. Sci Adv 2020;6(4):eaax3173.
[56] Kobayashi N, Nishino K, Yamaguchi A. Novel macrolide-specific ABC-type efflux transporter in *Escherichia coli*. J Bacteriol 2001;183(19):5639–44.
[57] Greene NP, Kaplan E, Crow A, Koronakis V. Antibiotic resistance mediated by the macb abc transporter family: a structural and functional perspective. Front Microbiol 2018;9:950.
[58] Heß S, Gallert C. Growth behavior of *E. coli*, *Enterococcus* and *Staphylococcus* species in the presence and absence of sub-inhibitory antibiotic concentrations: consequences for interpretation of culture-based data. Microb Ecol 2016;72(4):898–908.
[59] Gullberg E, Cao S, Berg OG, Ilbäck C, Sandegren L, Hughes D, et al. Selection of resistant bacteria at very low antibiotic concentrations. PLoS Pathog 2011;7(7):e1002158.
[60] Hall JPJ, Wright RCT, Harrison E, Muddiman KJ, Wood AJ, Paterson S, et al. Plasmid fitness costs are caused by specific genetic conflicts enabling resolution by compensatory mutation. PLoS Biol 2021;19(10):e3001225.
[61] Zhang J, Sui Q, Tong J, Zhong H, Wang Y, Chen M, et al. Soil types influence the fate of antibiotic-resistant bacteria and antibiotic resistance genes following the land application of sludge composts. Environ Int 2018;118:34–43.
[62] Udikovic-Kolic N, Wichmann F, Broderick NA, Handelsman J. Bloom of resident antibiotic-resistant bacteria in soil following manure fertilization. Proc Natl Acad Sci USA 2014;111(42):15202–7.
[63] Yang Y, Li B, Ju F, Zhang T. Exploring variation of antibiotic resistance genes in activated sludge over a four-year period through a metagenomic approach. Environ Sci Technol 2013;47(18):10197–205.
[64] Garner E, Chen C, Xia K, Bowers J, Engelthaler DM, McLain J, et al. Metagenomic characterization of antibiotic resistance genes in full-scale reclaimed water distribution systems and corresponding potable systems. Environ Sci Technol 2018;52(11):6113–25.
[65] Rutgersson C, Ebmeyer S, Lassen SB, Karkman A, Fick J, Kristiansson E, et al. Long-term application of Swedish sewage sludge on farmland does not cause clear changes in the soil bacterial resistome. Environ Int 2020;137:105339.
[66] Department for Environment Food & Rural Affairs. Fertiliser manual (RB209). 8th ed. Norwich: The Stationery Office (TSO); 2010.
[67] Wang F, Harindintwali JD, Yuan Z, Wang M, Wang F, Li S, et al. Technologies and perspectives for achieving carbon neutrality. Innovation 2021;2(4):100180.
[68] Tang M, Dou X, Tian Z, Yang M, Zhang Y. Enhanced hydrolysis of streptomycin from production wastewater using CaO/MgO solid base catalysts. Chem Eng J 2019;355:586–93.
[69] Lang Q, Zhang B, Liu Z, Chen Z, Xia Y, Li D, et al. Co-hydrothermal carbonization of corn stalk and swine manure: combustion behavior of hydrochar by thermogravimetric analysis. Bioresour Technol 2019;271:75–83.